Crystallographic and Computational Analysis of 4*H*-Pyran-3-Carboxylate Derivative Tethered with Amino and Methacryloyloxyethy l Units

Udhaya Kumar, Shunmugam Iniyaval, Kannan Gokula Krishnan, Muthiah Pillai Velayutham Pillai, Chennan Ramalingan

Abstract*: A single crystal of pyran derivative 1 was grown and analysed. The molecular structure of the same was theoretically executed through DFT approach. The frequencies and geometrical parameters obtained from computations are in good accord with the ones obtained through experimental. The calculated energies of HOMO and LUMO imply that transfer of charge happens within the molecule. Besides, the MEP analysis of the molecule 1 was examined using DFT calculations. X-Ray structural analysis (single crystal) of the molecule 1 implies that the pyran structural unit of the molecule adopts "flattened-boat" conformation.

Keywords: Crystal structure, Pyran derivative, DFT, HOMO-LUMO

I. INTRODUCTION

In recent years, great interests are shown towards the reactions under the category of multi-component, known as MCRs, in organic synthesis as well as medicinal chemistry domains.[1], [2] These methodologies provide a variety of advantages such as eco-friendliness, solvent-free strategies, atom economy, high selectivity, structural diversity, and good yields.[3]-[5] In particular, MCRs have been mostly applied in the synthesis of heterocyclic compounds.[6]-[8] Consequently, development of efficient and green reaction strategies focused on target molecules is a significant challenge in synthetic organic chemistry.[9], [10]

Revised Manuscript Received on December 17, 2019.
***** Correspondence Author
Chandran Udhaya Kumar, Department of Chemistry, School of Advanced Sciences, Kalasalingam Academy of Research and Education (Deemed to be University), Krishnankoil, 626 126, Tamilnadu, India. Email: udhayaachem86@gmail.com
Shunmugam Iniyaval, Department of Chemistry, School of Advanced Sciences, Kalasalingam Academy of Research and Education (Deemed to be University), Krishnankoil, 626 126, Tamilnadu, India. Email: iniyaval.s@klu.ac.in
Kannan Gokula Krishnan, Department of Chemistry, School of Advanced Sciences, Kalasalingam Academy of Research and Education (Deemed to be University), Krishnankoil, 626 126, Tamilnadu, India. Email: gokulskrishnank83@gmail.com
Muthiah Pillai Velayutham Pillai, Department of Chemistry, School of Advanced Sciences, Kalasalingam Academy of Research and Education (Deemed to be University), Krishnankoil, 626 126, Tamilnadu, India. Email: m.velayuthampillai83@klu.ac.in
***Chennan Ramalingan**, Department of Chemistry, School of Advanced Sciences, Kalasalingam Academy of Research and Education (Deemed to be University), Krishnankoil, 626 126, Tamilnadu, India. Email: ramalinganc@gmail.com

It is known that 4*H*-pyran and pyran-annulated ones are privileged heterocyclic structural cores because of the fact that many of their derivatives possess useful pharmacological properties[11], [12] and a wide range of biological profiles, which include antimalarial, anticancer, antimicrobial, anti-HIV, anti-inflammatory and cytotoxic etc. [13]-[18] Various methodologies have been developed for the construction of pyran ring systems. A few of novel methods include three component reaction utilizing a variety of catalysts such as piperidine,[19], [20] *S*-proline,[21] basic ionic liquid,[22] hydroxyapatite (HAP),[23] nano ZnO[24] and heteropolyacids.[25]

In this piece of research, we disclose a detailed investigation on crystallographic and computational studies of 4*H*-pyran-3-carboxylate derivative tethered with amino and methacryloyloxy)ethyl units **(1)**. Computational calculations were performed on novel 4*H*-pyran-3-carboxylate derivative **1** to explore its molecular structure and also to investigate the energy levels of HOMO and LUMO utilizing DFT. Computationally realized results of structural parameters (optimized) and vibrational assignments are evaluated with the ones resulted through experimental.

II. EXPERIMENTAL

A. Materials and methodologies

All starting materials / reagents / solvents were obtained from commercial suppliers and utilized as such with no additional purification. Melting point was recorded in open air capillary. XRD Data (single crystal) were acquired using a Bruker Kappa CCD diffractometer with Mo Kα (λ = 0.71073 Å) at room temperature. The title molecule **1** was synthesized by MCR strategy involving equimolar mixture of 2-(methacryloyloxy)ethyl 3-oxobutanoate, 3-bromo benzaldehyde and malononitrile in the presence of K_2CO_3 in water.

B. Structural studies (X-Ray) of novel 2-(methacryloyloxy)ethyl6-amino-4-(3-bromophenyl)-5-cyano-2-methyl-4H-pyran-3-carboxylate 1

A crystal of **1** was grown utilizing slow-evaporation methodology utilizing chloroform:ethanol mixture as a solvent system. Bruker,

2004 APEX 2 diffractometer with MoKα radiation (Kα = 0.71073 Å) at 293 K was used to collect diffraction data. Direct methods and successive Fourier difference synthesis (*SHELXS-97*) were utilized to solve the structure [26] and full matrix least square procedure on F^2 with anisotropic thermal parameters was used to refine the same. *SHELXL-97* was used to refine all non-hydrogen atoms.[27] The molecule novel 4*H*-pyran derivative **1** crystallizes in the triclinic system (*P*-1 space group) and there are two discrete compounds in the unit cell. There are 263 parameters refined with the number of unique reflections 3820 which roofed the residuals to R1= 0.0554. Mercury 3.5.1 and ORTEP-3 [28] softwares were used to arrange the material for publication. Crystallographic data of novel 4H-pyran derivative 1 are deposited in the CCDC (1842446).

C. Computational details

Theoretical calculation by single molecule approach was performed with a B3LYP [6-311++G (d,p)] method (gas phase) for all atoms within the framework of the DFT using the *Gaussian 09W* program.[29] The frequencies of vibrations calculated were scaled by 0.9679, a characteristic scaled factor for the calculated method.[30] The theoretical calculation yielded very closer prediction of the electronic and vibrational spectra as well as optimized geometry.

III. RESULTS AND DISCUSSION

A. Target 4H-pyran-3-carboxylate derivative 1

The target chemical entity 4*H*-pyran-3-carboxylate derivative **1** was synthesized by one-step three component reaction. A method of slow evaporation was adopted employing ethanol and chloroform as solvents to grow the single crystals.

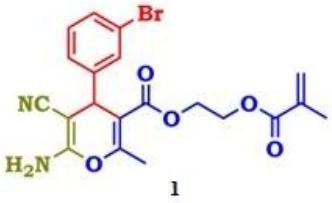

1

Figure 1

B. Structural and theoretical studies

C. X-Ray structural (single crystal) and optimized geometrical analysis of 4H-pyran derivative 1

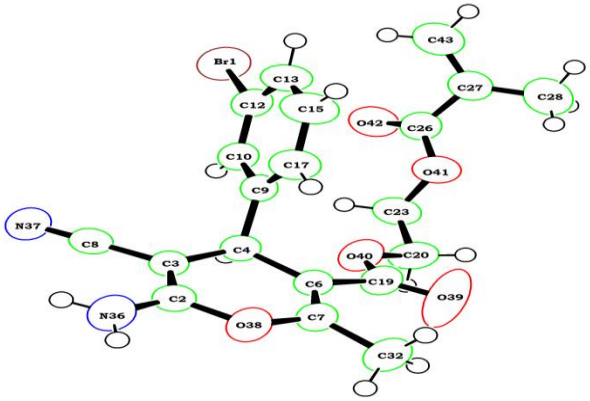

Fig. 2. ORTEP View of 4H-pyran derivative 1

The 4H-pyran derivative 1 crystallized in the system of triclinic with P-1 space group and the cell parameters correspond to, a = 8.2432(2) Å, b = 11.7555(3) Å, c = 12.2738(3) Å, α = 63.6170(10)°, β = 72.8740(10)°, γ = 71.711(2)° and Z = 2. The ORTEP view and packing diagram of the molecule 1 are shown in Fig. 2 and Fig. 3, respectively. Data of crystal and refinement features of structure of the molecule 1 are provided in Table I. The unity of crystal is realized through hydrogen bonds (intermolecular). The N-H···N≡C as well as N-H···O=C contacts possess bond distances of nearly 3.061 and 2.937 Å, respectively.

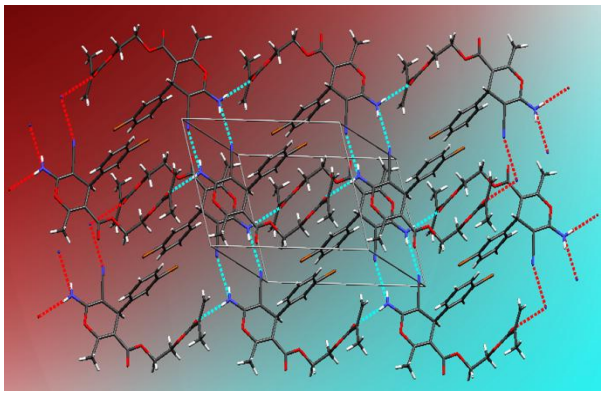

Fig. 3. Packing diagram of 4H-pyran derivative 1

Table - I

Crystallographic and Refinement Data of 4*H*-pyran derivative 1	
Empirical formula	C_{20} H_{19} Br N_2 O_5
Formula weight	447.28
Temperature	296(2) K
Wavelength	0.71073 Å
Crystal system, space group	Triclinic, P -1
Unit cell dimensions	a = 8.2432(2) Å α = 63.6170(10)° b = 11.7555(3) Å β = 72.8740(10)° c = 12.2738(3) Å γ = 71.711(2)°
Volume	994.72(4) $Å^3$
Z, Calculated density	2, 1.493 Mg/m^3
Absorption coefficient	2.100 mm^{-1}
F(000)	456
Crystal size	0.250 x 0.160 x 0.120 mm
Theta range for data collection	1.884 to 25.834°
Limiting indices	-10<=h<=9, -14<=k<=14, -15<=l<=15
Reflections collected / unique	14559 / 3820
Completeness to theta = 25.242	99.5 %
Refinement method	Full-matrix least-squares on F^2
Data / restraints / parameters	3820 / 0 / 263
Goodness-of-fit on F^2	1.054
Final R, R_W (obs, data)	0.0554, 0.1027

Table - IIa: Selected bond length (A°), bond angles (°) and torsion angles (°) of 4H-Pyran derivative 1

Torsion angle	Comp.	Expt.	Torsion angle	Comp.	Expt.
N36-C2-C3-C4	-179.796	175.1(3)	C7-C6-C19-O40	179.9866	167.5(2)
N36-C2-C3-C8	0.1764	-3.5(4)	C6-C7-O38-C2	32.4805	4.9(3)
O38-C2-C3-C4	0.3484	-4.3(4)	C32-C7-O38-C2	-147.661	-174.8(2)
O38-C2-C3-C8	-179.679	177.1(2)	C4-C9-C10-C12	-180	177.1(2)
C3-C2-O38-C7	-32.4817	-3.7(3)	C17-C9-C10-C12	0	-0.3(4)
N36-C2-O38-C7	147.6631	176.8(2)	C4-C9-C17-C15	179.9999	-177.6(3)
C2-C3-C4-C6	29.9816	9.7(3)	C10-C9-C17-C15	0.0002	-0.1(4)
C2-C3-C4-C9	-89.959	-114.5(3)	C9-C10-C12-Br1	180	-179.62(18)
C8-C3-C4-C6	-149.991	-171.7(2)	C9-C10-C12-C13	-0.0002	0.2(4)
C8-C3-C4-C9	90.0681	64.0(3)	Br1-C12-C13-C15	-180	-179.8(2)
C3-C4-C6-C7	-29.9828	-8.5(3)	C10-C12-C13-C15	0.0003	0.4(4)
C3-C4-C6-C19	149.9911	169.7(2)	C12-C13-C15-C17	-0.0001	-0.8(5)
C9-C4-C6-C7	89.958	114.9(2)	C13-C15-C17-C9	-0.0001	0.7(5)
C9-C4-C6-C19	-90.0681	-66.9(3)	C6-C19-O40-C20	-150	-172.5(2)
C3-C4-C9-C10	-90.3658	-106.0(2)	O39-C19-O40-C20	29.9997	8.1(4)
C3-C4-C9-C17	89.6345	71.4(3)	O40-C20-C23-O41	60.0001	83.4(3)
C6-C4-C9-C10	150.3653	131.6(2)	C23-C20-040-C19	179.9995	-154.8(2)
C6-C4-C9-C17	-29.6344	-50.9(3)	C20-C23-041-C26	-180	-170.9(2)
C4-C6-C7-C32	179.7949	-178.4(2)	O41-C26-C27-C28	-0.0001	39.5(4)
C4-C6-C7-O38	-0.3462	1.9(4)	O41-C26-C27-C43	179.9998	-141.9(3)
C19-C6-C7-C32	-0.179	3.5(4)	O42-C26-C27-C28	179.9996	-139.7(3)
C19-C6-C7-O38	179.6799	-176.2(2)	O42-C26-C27-C43	-0.0005	38.9(4)
C4-C6-C19-O39	-179.987	168.7(3)	C27-C26-041-C23	-150.001	5.0(4)
C4-C6-C19-O40	0.0128	-10.7(3)	O42-C26-O41-C23	29.9999	-174.3(2)
C7-C6-C19-O39	-0.0134	-13.1(4)			

Bond length	Comp.	Expt.	Bond length	Comp.	Expt.
Br1-C12	1.91	1.910(3)	C10-C12	1.3568	1.385(4)
C2-C3	1.3555	1.348(3)	C12-C13	1.3584	1.364(4)
C2-N36	1.47	1.331(4)	C13-C15	1.3568	1.373(4)
C2-O38	1.4384	1.367(3)	C15-C17	1.3998	1.389(4)
C3-C4	1.5318	1.509(3)	C19-O39	1.2584	1.188(3)
C3-C8	1.54	1.415(3)	C19-O40	1.43	1.323(3)
C4-C6	1.5318	1.521(3)	C20-C23	1.54	1.493(4)
C4-C9	1.54	1.531(3)	C20-O40	1.43	1.440(3)
C6-C7	1.3555	1.333(3)	C23-O41	1.43	1.442(3)
C6-C19	1.54	1.475(4)	C26-C27	1.54	1.478(4)
C7-C32	1.54	1.496(3)	C26-O41	1.43	1.335(3)
C7-O38	1.4384	1.380(3)	C26-O42	1.2584	1.199(3)
C8-N37	1.1466	1.141(3)	C27-C28	1.54	1.417(4)
C9-C10	1.3998	1.390(3)	C27-C43	1.3552	1.380(4)
C9-C17	1.352	1.371(4)			

Bond angle	Comp.	Expt.	Bond angle	Comp.	Expt.
C3-C2-N36	119.3316	128.0(2)	Br1-C12-C10	119.7821	122.1(2)
C3-C2-O38	121.3358	121.7(2)	Br1-C12-C13	119.782	119.13(19)
N36-C2-O38	119.3325	110.3(2)	C10-C12-C13	120.4359	122.1(2)
C2-C3-C4	119.8405	123.4(2)	C13-C15-C17	120.0059	120.2(3)
C2-C3-C8	120.0806	117.4(2)	C6-C19-O39	120.0001	126.7(2)
C4-C3-C8	120.0789	119.2(2)	C6-C19-O40	120	111.2(2)
C3-C4-C6	108.6241	109.03(18	O39-C19-O40	119.9999	122.1(3)
C3-C4-C9	109.722	110.9(2)	C23-C20-O40	109.4714	107.6(2)
C6-C4-C9	109.7219	112.33(19	C20-C23-O41	109.4712	107.2(2)
C4-C6-C7	119.8405	122.8(2)	C27-C26-O41	120	112.0(2)
C4-C6-C19	120.0797	117.6(2)	C27-C26-O42	120.0001	125.7(2)
C7-C6-C19	120.0797	119.6(2)	O41-C26-O42	119.9999	122.2(2)
C6-C7-C32	119.332	129.4(2)	C26-C27-C28	120	118.2(3)
C6-C7-O38	121.3356	122.5(2)	C26-C27-C43	120	117.1(3)
C32-C7-O38	119.3322	108.1(2)	C28-C27-C43	120	124.7(3)
C4-C9-C10	120.221	120.0(2)	C2-O38-C7	112.7655	119.62(18)
C4-C9-C17	120.2207	120.8(2)	C19-O40-C20	109.4714	118.2(2)
C10-C9-C17	119.5582	119.1(2)	C23-O41-C26	109.4711	116.6(2)
C9-C10-C12	120.0058	119.0(3)			

The geometry of optimized molecule **1** was computed by DFT-B3LYP [6-311++G (d,p)] method. The molecular structure along with numbering of atoms of **1** is provided in **Fig. 4** and the selected experimental and theoretical torsion angles, bond angles and bond lengths are depicted in **Table II**

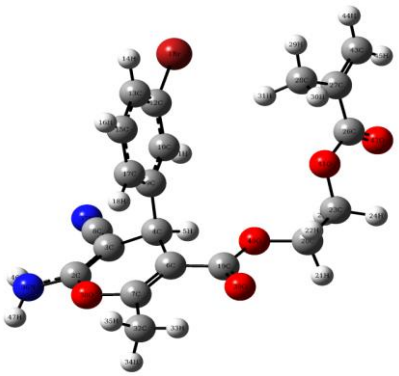

Fig. 4. Optimized Structure of 4H-pyran derivative 1

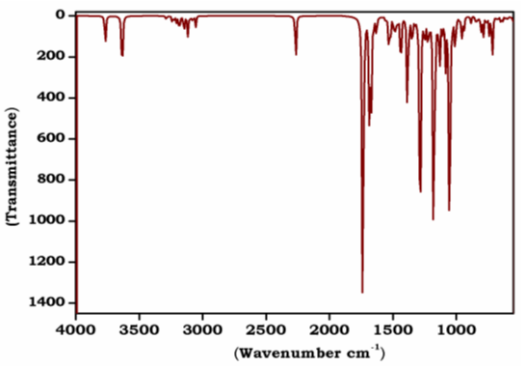

Fig. 5. Theoretical IR spectra of 1.

X-Ray structural (single crystal) and optimized geometrical analysis of the molecule **1** reflects the conformation of pyran ring scaffold is "*flattened boat*". This conformation is validated from the parameters of small puckering related with the atoms O(38) and C(4). The aforesaid atoms available at 1 and 4 positions of the pyran nucleus, which are displaced by (XRD/DFT) 0.044 / 0.127 and 0.116 / 0.266 Å, respectively from the plane defined by C(2)/C(3)/C(6)/C(7). The structural core of aryl is virtually vertical to the structural core of pyran with the angle of (XRD/DFT) 110.89 / 112.47°.

In the pyran scaffold, a couple of bonds such as C(6)-C(7) and C(2)-C(3) possess multiple bond (double bond) nature as shown in their bond distances [XRD/DFT; C(2)-C(3)= 1.348 / 1.363 and C(6)-C(7)=1.333 / 1.355 Å]. The parameters of bond related with the ester moiety (**Table II**) evidently indicate the density of partial π-electron delocalization over COO^{-} unit and, the nitrile functionality is just about linear [XRD/DFT; N(37)-C(8)-C(3)= 179.4 / 179.2°] and multiple bonded (triple bonded) in nature as well [XRD/DFT; C(8)-N(37)= 1.14 / 1.17 Å]. The incorporation of halogen decreases the density of electrons at the carbon atoms present in the phenyl ring. The C(12)-Br(1) bond length is found to be (XRD/DFT) 1.91 / 1.910 Å.

In the side arm, bonds of C(19)-O(39) and C(26)-O(42) are in the double-bonded environment as shown by the distances between them [XRD/DFT; C(19)-O(39)= 1.188 / 1.242 and C(26)-O(42)=1.199 / 1.239 Å]. Besides, the bond C(27)-C(28) is also double-bonded in character as shown by the distance between them [XRD/DFT; C(27)-C(28)= 1.417 / 1.344 Å]. The optimized bond and torsion angles as well as bond lengths are in fine conformity with the structural parameters of X-ray of the title compound 1.

D. IR spectral analysis of novel 4H-pyran derivative 1

The computational infrared spectra of 4*H*-pyran derivative **1** is displayed in **Fig. 5**.

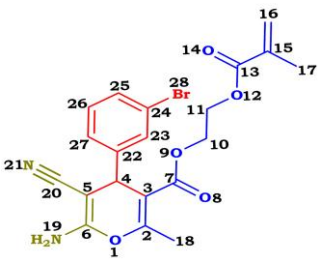

The stretching vibrations of C-H in the aromatic ring usually appear nearly from 3100 to 3000 cm-1 [31]. The vibrations (stretching) of C-H in the aryl ring are theoretically obtained at 3203, 3190, 3187 and 3170 cm-1. Further, the stretching vibrations of C-H in the aliphatic region are theoretically observed at 3062, 3053, 3036 and 3032 cm-1. The computed vibrational frequencies (unscaled and scaled) are presented in Table III.

In the FT-IR spectrum, the C=O group with various environments generally appear as a strong band in the range between 1800-1600 cm^{-1}[31], [32]. In the 4*H*-pyran derivative **1**, the C=O stretching vibrations of O14=C13, attached to carbon containing olefin and methyl group and O8=C7, connected to pyran molecule are theoretically resulted at 1777 and 1763 cm^{-1}, respectively.

Besides, the nitrile groups normally provide unique spectral values and gives intense absorption between 2280 and 2200 cm^{-1}. As a result of theoretical calculation at B3LYP level, the stretching vibration of nitrile functionality is observed at 2299 cm^{-1}. Additionally, the existence of an amine (primary) functionality usually shows vibrations (stretching) of N-H in the range between 3400 and 3300 cm^{-1}. The theoretical spectrum of FT-IR of 4*H*-pyran derivative **1** depicts two typical bands at 3686 and 3573 cm^{-1}.

Further, in most of the bromoaryl molecules, the stretching vibrations of C-Br present in the range between 650 and 395 cm^{-1}[32]. In the simulated spectrum of 4*H*-pyran derivative **1**, the aromatic C-Br stretching vibrations appeared at 679 cm^{-1}.

Table- III: Selected simulated FT-IR spectral data of 4*H*-pyran derivative 1

Mode	Unscaled	Scaled	Intensity	Assignment
1	446	431	53.4	rC17C15C13C12(29); τBr1C10C13C12(18); rH16C15C17C9(14)
2	496	479	11.09	βN36C2O38(11); βN37C8C3(10); rN37C8C3C4(10)
3	514	497	2.64	βC27C26O41(20); βO41C23C20(17); βC28C27C26(15)
4	679	657	12.71	βC17C15C13(18); νB1rC12(16); τN36C3O38C2(14); βC13C12C10(12)

5	710	686	7.14	τN36C3O38C2(18)
6	754	729	29.34	τO39C6O40C19(34); νC32C7(10)
7	886	857	12.84	νO40C20(22); rH24C23O41C26(14); νC23C20(10)
8	911	881	6.87	νC28C27(15); νO41C23(14); rH14C13C15C17(11); rH18C17C9C4(10)
9	969	937	23.41	βH44C43C27(26); νC28C27(13)
10	1117	1080	15.71	βH14C13C15(22); νC17C15(17); νC12C10(12); νC13C12(12); βH18C17C9(10)
11	1140	1102	100	νC6C4(19); νC32C7(12)
12	1357	1312	12.54	rH5C4C9C10(26); βH5C4C9(21)
13	1394	1348	45.37	rH21C20O40C19(20); rH24C23O41C26(19); rH25C23O41C26(12); rH22C20O40C19(11)
14	1420	1373	7.71	νN36C2(22); βC3C2O38(15); βH35C32H34(10)
15	1436	1389	18.46	βH45C43H44(33); βH31C28H30(18)
16	1453	1405	19.8	βH18C17C9(22); βH14C13C15(15); βH5C4C9(12); νC12C10(10)
17	1504	1455	27.59	βH16C15C17(26); βH11C10C9(18); νC13C12(10); βH14C13C15(10)
18	1607	1554	44.69	νC15C13(30); νC9C17(18); βC13C12C10(11); βC9C17C15(11)
19	1763	1705	55.97	νO39C19(77)
20	1777	1719	34.45	νO42C26(83)
21	2299	2223	17.73	νN37C8(88); νC8C3(12)
22	3170	3066	10.46	νC15H16(68); νC17H18(27)
23	3190	3085	2.9	νC10H11(98)
24	3203	3097	8.42	νC13H14(88); νC15H16(10)
25	3238	3131	6.24	νC43H45(59); νC43H44(41)
26	3573	3455	39.47	νN36H46(50); νN36H47(50)
27	3686	3564	27.33	νN36H46(50); νN36H47(50)

E. Mulliken population analysis of 4H-pyran derivative 1

The charge distributions (total) of 4H-pyran derivative 1, derived from the Mulliken methodology are given in Table IV. The symbolic depiction of distribution of Mulliken charge is furnished in Fig. 6 and the equivalent plot is given in Fig. 7. A survey of mulliken plot of 4H-pyran derivative 1 reveals that the molecule has relatively higher number of nucleophilic centres. The electrophilic behaviour is pronounced only to a limited number of atoms viz., C3 (1.05), C6 (1.28), C9 (0.62), C17 (0.21) and C27 (0.63) and their electrophilicity ranges from 0.21 (C17) to 1.28 (C6). Further, the electrophilic nature of the atoms is ascribable to the fact that they are attached to electron withdrawing neighbours such as C2 (-0.51), C7 (-0.55), C8 (-0.74), C19 (-0.55), C28 (-0.60) and C43 (-0.37).

Table- IV: Mulliken Atomic Charges for 4*H*-pyran derivative 1

Atom	Atomic Charge	Atom	Atomic Charge
1Br	-0.13373	20C	-0.18059
2C	-0.51371	23C	-0.27579
3C	1.054296	26C	-0.23713
4C	-0.23602	27C	0.637876
6C	1.281876	28C	-0.60541
7C	-0.55784	32C	-0.4503
8C	-0.74582	36N	-0.31659
9C	0.625856	37N	-0.20045
10C	-0.40154	38O	-0.07609
12C	-0.07612	39O	-0.1779
13C	-0.23523	40O	-0.00289
15C	-0.39832	41O	-0.05609
17C	0.219406	42O	-0.25511
19C	-0.55863	43C	-0.37055

The charge transfer probably occurs significantly in the following pairs as per the observation: C3→C8, C6→C19 and C6→C7, C9→C10, C17→C15, C27→C28 and C27→C43. It is also noted that some of the atoms show neither electrophilic nor nucleophilic tendencies to an appreciable level. On inspection, the atoms Br1, C12, O38, O40 and O41 are found to possess less charge than the expected values.

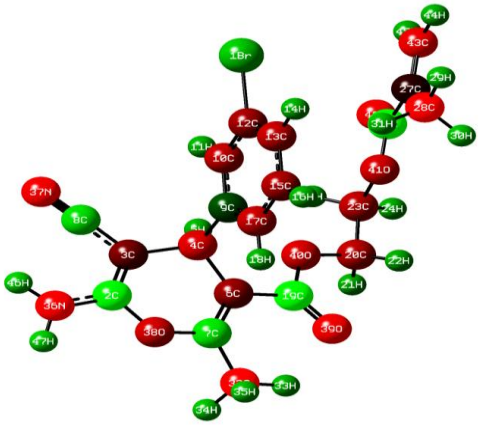

Fig. 6. Mulliken charge distribution of 4H-pyran derivative 1

Fig. 7. Mulliken atomic charges for 4H-pyran derivative 1

F. Molecular electrostatic potential of 4H- pyran derivative 1

Electrostatic Potential mapping normally provides a visual scheme to classify the comparative polarity of a compound. **Fig. 8** exhibits the MEP surface plot for 4*H*-pyran derivative **1**. The divergent electrostatic potential values on the surface are assigned by diverse range of colors; blue indicates most positive regions, red represents most negative regions, and green points out zero potential.

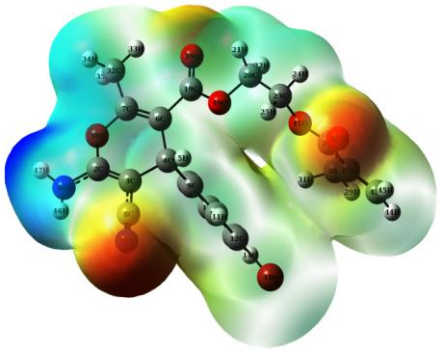

Fig.8. MEP mapping of 4H-pyran derivative 1

The classification of increasing potential is, red < orange < yellow < green < blue. The nucleophiles tend to the positive and the electrophiles tend to the negative. The carbonyl groups C18=O29, C26=O42 and cyano group C8≡N37 of title compound **1** have more electron density as the region around them appears red and they are being the possible sites for electrophilic attack. The nitrogen atom of amino group (N36) is represented by blue colour and being a possible site for nucleophilic attack.

G. FMO analysis of 4H-pyran derivative 1

The difference in energy between HOMO and LUMO generally elucidates the charge switchover in a molecule and clarifies the chemical and biological activities of a molecule. If the difference in energy between HOMO and LUMO is found to be large, the molecule possesses more stability and hence the reactivity would be less. The energies of FMO and their difference for the 4*H*-pyran derivative **1** are tabulated in **Table V**. In the case of molecule **1**, the electrons of HOMO are delocalized over phenyl ring only (**Fig. 9**), while the electrons of LUMO are delocalized over carbonyl and methylene groups.

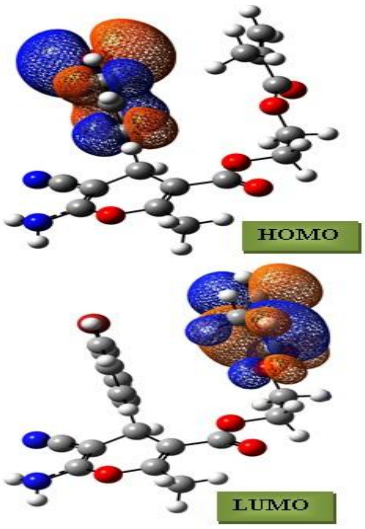

Fig. 9. HOMO-LUMO plot of 4H-pyran derivative 1

Table- V: Calculated HOMO-LUMO energies of 4*H*-pyran derivative 1

Parameters	Energies (ΔE)	Band Gap (a.u)
HOMO	0.07074	0.16822
LUMO	0.23896	

IV. CONCLUSION

Single crystal of target molecule 1 has been grown by adopting slow evaporation methodology. Complete structural and vibrational properties of the same have been analysed by adopting computational and single crystal x-ray diffraction studies. The MEP visibly exposes the existence of more positive charge around the amino moiety. The FMO calculated energies reflect the occurrence of charge transfer within the molecule. XRD analysis (single crystal) of the molecule 1 supports the "flattened boat" conformation of the pyran moiety.

ACKNOWLEDGMENT

Financial assistance provided by the Indian Council of Medical Research, New Delhi (No.58/16/2013BMS) and Kalasalingam Academy of Research and Education (PDF to CU and KG) Anand nagar, India is gratefully acknowledged.

REFERENCES

1. M. C. Pirrung, K. D. Sarma, "Multicomponent Reactions Are Accelerated in Water", *J. Am. Chem. Soc*, vol. 126, pp. 444-445, 2004.
2. E. Ruijter, R. V. A. Orru, "Multicomponent reactions – opportunities for the pharmaceutical industry", *Drug Discovery Today: Technologies, vol*. 10, pp. 15-20, 2013.
3. M. K. Ghorai, R. Talukdar, D. P. Tiwari, "An efficient synthetic route to carbocyclic enaminonitriles via Lewis acid catalysed domino-ring-opening-cyclisation (DROC) of donor-acceptor cyclopropanes with malononitrile", *Chem. Commun*, vol. 49, pp. 8205-8207, 2013.
4. Y. Hayashi, "Pot economy and one-pot synthesis", *Chem. Sci*, vol. 7, pp. 866-880, 2016.

5. S. Nagaraju, K. Sathish, B. Paplal, D. Kashinath, "On-water" catalyst-free, one pot synthesis of quaternary centered and spiro-tetrahydrothiophene-barbiturate hybrids", *Tetrahedron Lett*, vol. 58, pp. 2865-2871, 2017.
6. D. Srikrishna, P. K. Dubey, "PEG-600 mediated one-pot reaction of 3-acetyl-2H-chromene-2-one with heterylthiols and phenylthioureas using tetrabutylammonium tribromide as an efficient green reagent", *New J. Chem*, vol. 41, pp. 5168-5175, 2017.
7. G. Dupeyre, P.Lemoine, N. Ainseba, S. Michel, X. Cachet, "A one-pot synthesis of 7-phenylindolo[3,2-a] carbazoles from indoles and β-nitrostyrenes, via an unprecedented reaction sequence", *Org. Biomol. Chem*, vol. 9, pp. 7780-7790, 2011.
8. S. Huang, Y. Pan, Y. Zhu, A. Wu, " A Novel Three-Component One-Pot Reaction Involving Alkynes, Urea or Thiourea and Aldehydes", *Org. Lett*, vol. 7, pp. 3797-3799, 2005.
9. C. Ramalingan, S. J. Park, I. S. Lee, Y. W. Kwak, "A piperidinium triflate catalyzed Biginelli reaction", *Tetrahedron*, vol. 66, pp. 2987-2994, 2010.
10. C. Ramalingan, Y. W. Kwak, "Tetrachlorosilane catalyzed multicomponent one-step fusion of biopertinent pyrimidine heterocycles", *Tetrahedron*, vol. 64, pp. 5023-5031, 2008.
11. S. W. Youn, E. M. Lee, "Metal-Free One-Pot Synthesis of N,N'-Diarylamidines and N-Arylbenzimidazols from Arenediazonium salts, Nitriles, and Free Anilines", *Org. Lett*, vol. 18, pp. 5728-5731, 2016.
12. M. Zangouei, A. A. Esmaeili, J. T. Mague, "One-pot three component isocyanide-based reaction: Synthesis of novel tetracyclic fused furo[2',3':4,5] pyrimido[2,1-b][1,3]benzothiazole", *Tetrahedron*, vol. 73, pp. 2894-2900, 2017.
13. J. L. Wang, D. Liu, Z. J. Zhang, S. Shan, X. Han, S. M. Srinivasula, C. M. Croce, E. S. Alnemri, Z. Huang, "Structure-based discovery of an organic compound that binds Bcl-2 protein and induces apoptosis of tumor cells", *Proc. Natl. Acad. Sci., USA* vol. 97, pp 7124-29, 2000.
14. Y. Peng, G. Song, "Amino-functionalized ionic liquid as catalytically active solvent for assisted synthesis of 4H-pyrans", Catal. Commun, vol. 8, pp. 111-114, 2007.
15. J. Y. C. Wu, W. F. Fong, J. X. Zhang, C. H. Leung, H. L. Kwong, M. S. Yang, D. Li, H. Y. Cheung, "Reversal of multidrug resistance in cancer cells by pyranocoumarins isolated form Radix Peucedani", *Eur. J. Pharmacol*, vol. 473, pp. 9-17, 2003.
16. T. Raj, R. K. Bhatia, A. Kapur, M. Sharma, A. K. Saxena, M. P. S. Ishar, "Cytotoxic activity of 3-(5-phenyl-3H-[1,2,4]dithiazol-3-yl)chromen-4-ones and 4-oxo-4H-chromene-3-carbothioic acid N-phenylamides", Eur. *J. Med. Chem*, vol. 45, pp. 790-794, 2010.
17. M. T. Flavin, J. D. Rizzo, A. Khilevich, A. Kucherenko, A. K. Sheinkman, V. Vilaychack, L. Lin, W. Chen, E. M. Greenwood, T. Pengsuparp, J. M. Pezzuto, S. H. Hughes, T. M. Flavin, M. Cibulski, W. A. Boulanger, R. L. Shone, Z. Q. Xu, "Synthesis, chromatographic resolution and anti-human immunodeficiency virus activity of (+/-) – calanolide A and its enantiomers", *J. Med. Chem*, vol. 39, pp. 1303-1313, 1996.
18. D. O. Moon, K. C. Kim, C. Y. Jin, M. H Han, C. Park, K. J. Lee, Y. M. Park, Y. H. Choi, G. Y. Kim, "Inhibitory effects of eicosapentaenoic acid on lipopolysaccharide-induced activation in BV2 microglia", *Int. Immunopharmacol*, vol. 7, pp. 222-229, 2007.
19. E. Perez-Sacau, A. Estevez-Braun, A. G. Ravelo, D. G. Yapu, A. G. Turba, "Antiplasmodial Activity of Naphthoquinones Related to Lapachol and β-Lapachone", *Chem. Biodiversity*, vol. 2, pp. 264-274, 2005.
20. L. R. Morgan, B. S. Jursic, C. L. Hooper, D. M. Neumann, K. Thangaraj, B. Leblance, "Anticancer activity for 4,4'-Dihydroxybenzophenone-2,4-dinitrophenylhydrazone (A-007) analogues and Their abilities to interact with lymphoendothelial cell surface markers", *Bioorg. Med. Chem. Lett*, vol. 12, pp. 3407-3411, 2002.
21. T. Akbarzadeh, A. Rafinejad, J. M. Mollaghasem, M. Safari, A. F. Tafti, M. Pordeli, S. K. Ardestani, A. Shafiee, A. Foroumadi, "2-Amino-3-cyano-4-(5-arylisoxazol-3-yl)-4H-chromenes: Synthesis and In Vitro Cytotoxic Activity", *Arch. Pharm. Chem. Life Sci*, vol. 345, pp. 386-392, 2012.
22. M. Mahmoodi, A. Aliabadi, S. Emami, M. Safavi, S. Rajabalian, M. Mohagheghi, A. Khoshzaban, A. Samzadeh-Kermani, N. Lamei, A. Shafiee, A. Foroumadi, "Synthesis and in-vitro Cytotoxicity of Poly-functionalized 4-(2-Arylthiazol-4-yl)-4H-chromenes", *Arch. Pharm. Chem. Life Sci*, vol. 343, pp. 411-416, 2010.
23. S. Abdolmohammadi, S. Balalaie, "Novel and efficient catalysts for the one-pot synthesis of 3,4-dihydropyrano[c]chromene derivatives in aqueous media", *Tetrahedron Lett, vol*. 48, pp. 3299-3303, 2007.
24. K. Gong, H. L. Wang, J. Luo, Z. L. Liu, "One-pot synthesis of polyfunctionalized pyrans catalyzed by basic ionic liquid in aqueous media", *J. Heterocycl. Chem*, vol. 46, pp. 1145-1150, 2009.
25. Y. Essamlali, O. Amadine, H. Maati, K. Abdelouahdi, A. Fihri, M. Zahouily, R. S. Varma, A. Solhy, "Highly efficient one-pot three-component synthesis of naphthopyran derivatives in water catalyzed by phosphates", *ACS Sustainable Chem*. Eng, vol. 1, pp. 1154-1159, 2013.
26. G. Sheldrick, "A short history of SHELX", *Acta Crystallogr. Sect. A*, vol. 64, pp. 112-122, 2008.
27. L. J. Farrugia, "WinGX suite for small-molecule single-crystal crystallography", *J. Appl. Crystallogr*, vol. 32, pp. 837-838, 1999.
28. L. J. Farrugia, *J. Appl. Crystallogr*, vol. 30, pp. 565−566, 1997.
29. T. Vreven, K. N. Kudin, J. C. Burant, J. M. Millam, S. S. Iyengar, J. Tomasi, V. Barone, B. Mennucci, M. Cossi, G. Scalmani, N. Rega, G. A. Petersson, H. Nakatsuji, M. Hada, M. Ehara, K. Toyota, R. Fukuda, J. Hasegawa, M. Ishida, T. Nakajima, Y. Honda, O. Kitao, H. Nakai, M. Klene, X. Li, J. E. Knox, H. P. Hratchian, J. B. Cross, V. Bakken, C. Adamo, J.Jaramillo, R. Gomperts, R. E. Stratmann, O. Yazyev, A. J. Austin, R. Cammi, C. Pomelli, J. W. Ochterski, P. Y. Ayala, K. Morokuma, G. A. Voth, P. Salvador, J.J. Dannenberg, V. G. Zakrzewski, S. Dapprich, A. D. Daniels, M. C. Strain, O. Farkas, D. K. Malick, A. D. Rabuck, K. Raghavachari, J. B. Foresman, J. V. Ortiz, Q. Cui, A. G. Baboul, S. Clifford, J. Cioslowski, B. B. Stefanov, G. Liu, A. Liashenko, P. Piskorz, I. Komaromi, R. L. Martin, D. J. Fox, T. Keith, M. A. Al-Laham, C. Y. Peng, A. Nanayakkara, M. Challacombe, P. M. W. Gill, B. Johnson, W. Chen, M. W. Wong, C. Gonzalez, J. A. Pople, Gaussian 09, Revision C.02; Gaussian, Inc., Wallingford CT 2004.
30. M. H. Jomroz, Vibrational Energy Distribution Analysis, VEDA4, Warsaw, 2004.
31. G. Socrates, Infrared and Raman Characteristic Group Wave Numbers – Tables and Charts, third ed., John Wiley and sons, New York, (2001).
32. V. Arjunan, S. Thirunarayanan, S. Mohan, "Energy profile, spectroscopic (FT-IR, FT-Raman and FT-NMR) and DFT studies of 4-bromoisophthalic acid", *J. Mol. Struct*, vol. 1157, pp. 132-148, 2018.

AUTHORS PROFILE

Dr. Chandran Udhaya Kumar Graduated from Thyagaraja College, Madurai (2009) and pursued doctoral research in Organic Chemistry at Annamalai University (2014). He then served as postdoctoral fellow at Kalasalingam Academy of Research and Education, Krishnankoil, India (2015-2018). He published 24 research articles in peer-reviewed journals. His areas of research are Organic Synthesis, X-ray crystallography and Computational Chemistry.

Shunmugam Iniyaval obtained her Bachelor of Science degree in Chemistry from Sri Parasakthi College for Women, Courtrallam in 2013. She earned her Master's degree in Chemistry in 2015 from Sri Paramakalyani College, Alwarkuruchi. She is currently a PhD student at Kalasalingam Academy of Research and Education, Krishnankoil. She has been working in the area of heterocyclic synthesis and medicinal chemistry.

Dr. Kannan Gokula Krishnan Graduated from Sacred Heart College, Thiruppathur (2009) and completed his doctoral degree in Organic Chemistry at Annamalai University (2015). He then prosecuted his postdoctoral research at Kalasalingam Academy of Research and

Education, Krishnankoil, India (2015-2018). He published 10 research articles in peer-reviewed journals. His areas of research are Organic Synthesis, development of biopertinent molecules and Computational Chemistry.

Dr. Muthiah Pillai Velayutham Pillai had his graduation from Christian College, Nagercoil (1997) and earned his doctoral degree from Annamalai University (2014). Presently, he is serving as Assistant Professor of Chemistry at Kalasalingam Academy of Research and Education, Krishnankoil, India. His areas of research are Organic Synthesis, Crystallography ad Computational Chemistry. He published 14 research articles in peer-reviewed journals.

Dr. Chennan Ramalingan is serving as Professor of Chemistry at KARE. He received his PhD in Organic Chemistry from Annamalai University (2002). After he served as Research Professor at Kyungpook National University, South Korea followed by Assistant Professor at Osaka University, Japan (8 years), he joined at Kalasalingam Academy of Research and Education, Krishnankoil (2011). His research interests include organic synthesis, medicinal chemistry and material chemistry. He published more than 70 International research articles.